

Microdevice for Separation of Circulating Tumor Cells using Embedded Magnetophoresis with v-shaped Ni-Co Nanowires and Immuno-nanomagnetic Beads

Jeong Won Park, Nae Lim Lee, Sung Mok Cho, Moon Youn Jung, Chunhwa Ihm, and Dae-Sik Lee

The novelty of this study resides in a 6'-wafer-level microfabrication protocol for a microdevice with a fluidic control system for the separation of circulating tumor cells (CTCs) from human whole blood cells. The microdevice utilizes a lateral magnetophoresis method based on immunomagnetic nanobeads with anti-epithelial cell adhesive molecule (EpCAM) antibodies that selectively bind to epithelial cancer cells. The device consists of a top polydimethylsiloxane (PDMS) substrate for microfluidic control and a bottom substrate for lateral magnetophoretic force generation with embedded magnetic microwires, all using micromachining processes. We designed embedded v-shaped soft magnetic wires for the bottom substrate for more efficient microfluidic separation of the CTCs. The processes used can be mainly characterized as the electroplating of 100 μm -wide and 60 μm -thick Nickel-Cobalt (Ni-Co) soft magnetic wires, chemical mechanical polishing (CMP), and hermetic sealing between the PDMS and SU-8. First, we describe the observation of CTC isolation rates as a function of the external static magnetic intensity. Next, we demonstrate that the microdevice can isolate about 93% of the spiked cancer cells (MCF-7, a breast cancer cell line) in whole human blood at a flow rate of 40/100 $\mu\text{L}/\text{min}$ with respect

to a whole human blood/buffer solution. For the overall isolation, it takes only 10 min to process and analyze 400 μL of whole human blood. The fabrication method is sufficiently cheap, simple, and easy, allowing the proposed microdevice to be a practical and mass-producible clinical tool for cancer diagnosis, prognosis, and personalized medicine.

Keywords: Breast cancer, Circulating Tumor Cells, Ni-Co electroplating, Microfluidic, Cancer Diagnosis.

I. Introduction

Hematogeneous tumor cell dissemination is a key step in cancer metastasis. Thus, the detection of circulating tumor cells (CTCs) in the peripheral blood of patients with solid epithelial tumors can provide the opportunity for the early detection of cancer metastasis, and CTC detection has been reported to be a less invasive cancer prognosis after surgery because the number of CTCs is strongly related with the survival rates of the patients [1]-[8]. For decades, many exciting technologies for CTC detection have been developed. Among them, CellSearch®, a technology based on EpCAM positive enrichment, has received US FDA approval for CTC detection as an aid in monitoring patients with metastatic breast, colorectal, or prostate cancer [1], [4]-[5]. However, the detection and molecular characterization of CTCs still remain technically challenging. Because CTCs are present at very low concentrations in peripheral blood (less than 10 cells per mL of normal blood), the identification and characterization of CTCs require extremely sensitive and specific analytical methods, which are usually a combination of complex enrichment and detection procedures.

Microfluidic and microfabrication methods allow developed microdevices to be used for the separation of CTCs and the following analyses [9]-[10]. By monitoring images, ion

Manuscript received May 12, 2014; revised Dec. 1, 2014; accepted Dec. 8, 2014.

The Si-based devices fabrication was performed at the ETRI CMOS fab. and MEMS Laboratory. This work was supported by the Ministry of Knowledge and Economy, Korea (2010-S-007-04, Ubiquitous Health Monitoring Module and System Development) and the Ministry of Science, ICT, and Future Planning (2013-M3C8A1078454, Development of Liquid Biopsy Device technology for companion diagnostics) through NRF, Korea.

Chunhwa Ihm (haneul@eulji.ac.kr) is with Department of Laboratory Medicine, Eulji University Hospital, Daejeon, Rep. of Korea.

Jeong Won Park (jwp0422@etri.re.kr), Nae Lim Lee (infinity@etri.re.kr), Sung Mok Cho (smcho@etri.re.kr), Moon Youn Jung (myjung@etri.re.kr), and Dae-Sik Lee (corresponding author, dslee@etri.re.kr) is with the Industry-Strategy Research Department, ETRI, Daejeon, Rep. of Korea.

currents, and force as cells isolate through a solid-state microdevice, it is possible to observe a wide range of phenomena involving cancer prognosis, diagnosis of minimal residual diseases, the assessment of tumor sensitivity to anticancer drugs, and the personalization of anticancer medicines [1], [9]-[11]. Solid-state microdevices have proven to be very versatile tools for the separation of CTCs.

Owing to its good isolation and excellent purification performance [9],[12]-[14], a magnetic activated cell sorter (MACS) is one promising method that allows high-throughput separation of magnetically labeled target species as compared to other label-free separation processes, such as dielectrophoresis-based, size-based, or hydrophoresis-based cell isolation [15]-[18]. However, there is still a strong need to enhance the separation performance to reduce the loss, elevate the purity, and shorten the analysis time for use in real clinical applications [8], [12]. To do so, a microfluidic design that reduces the loss and the development of a new microfabrication protocol are needed, not only with the more enhanced magnetic materials and their structures but also using a low cost, simple, and mass-producible method. For this purpose, the Ni-Co system is known to have advantages over other systems because, depending on the Co content, its magnetic characteristics have been reported to shift from soft magnetic for a low Co content to permanent magnetic for higher Co containing alloys, possibly maintaining compatibility with mass-producible micromachining technologies [1519]-[1721].

Herein, we describe a new CTC separation device based on lateral magnetophoresis characterized as a 60 μm -thick and 100 μm -wide Ni-Co soft magnetic wire array inlaid on the bottom of a glass substrate to enhance the magnetic force affecting the target cells. The magnetic film process is compatible with standard MEMS fabrication technology, making it possible to be included in the batch process. Furthermore, we also designed a lab-made fluidic control system for an integrated diagnostic instrument. We investigated the effect of external static magnetic intensity on the separation rates. In addition, we demonstrated that the microdevices separated about 93% of the spiked CTCs cancer cells (MCF-7) in whole human blood at a flow rate of 40/100 $\mu\text{L}/\text{min}$ with respect to a blood/buffer solution using a 400 μL of whole human blood within a 10 min period.

II. Experimental

1. Microdevice design for CTC separation

We designed and fabricated the microdevice for the separation of CTCs from whole human blood based on a lateral magnetophoresis principle and nano-sized

immunomagnetic beads with the EpCAM antibodies that selectively bind to epithelial cancer cells (MCF-7, a breast cancer cell line), as shown in Fig. 1. The separation is stimulated by a magnetic field gradient-based force using a lateral magnetophoresis method. In particular, a Ni-Co soft magnetic thick film has been utilized. Easy deposition, full compatibility with a variety of MEMS fabrication processes (surface as well as bulk fabrication technologies), good adherence, a solid solution ensuring the homogeneity of the layer, and a high magnetic response (even in a few micrometer-thick layers) are well known benefits [15]-[17].

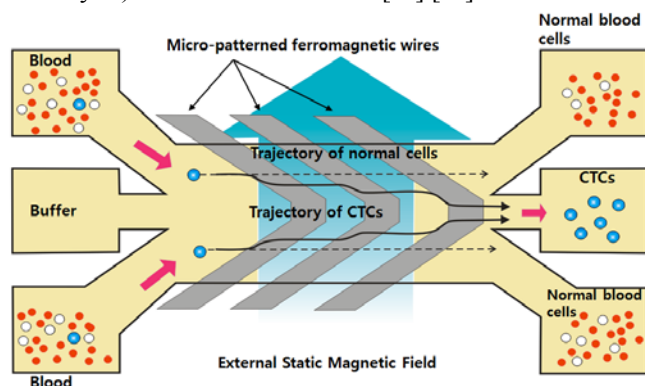


Fig. 1. Schematic diagram showing the working principles of a microdevice for separation of CTCs using lateral magnetophoresis and immunomagnetic nanobeads.

We designed the device so that cells flow over a region of integrated microfabricated ferromagnetic stripes (Fig. 1). The magnetic field pattern from each stripe creates a magnetic trap that alters the movement of only those cells coated with superparamagnetic beads. Cells with a sufficient quantity of magnetic nanobeads become trapped over the magnetic stripes and move only along the stripe direction, not parallel to the fluid flow. Quantitatively, the magnetic force \mathbf{F}_m on a particle with a saturated magnetic dipole \mathbf{M}_s in magnetic field \mathbf{B} is

$$\vec{F}_m \approx \left| \vec{M}_s \right| \nabla \vec{B} \quad (1)$$

The beads used in our case are superparamagnetic, leading to a saturation of the magnetization at relatively low magnetic fields of 0.01 T, and negligible remanence. Thus, \mathbf{M}_s for fields greater than 0.01 T can be treated as a vector quantity of constant magnitude, but parallel to \mathbf{B} , and the force becomes

$$\vec{F}_m \approx S \mu_0 \mu_B \nabla B, \quad (2)$$

where S is the number of Bohr magnetons μ_B per bead, μ_0 is the permeability of free space, and B is the magnitude of the

magnetic field. The magnetically labeled cell is subject to both a magnetic force in the vertical direction and a magnetic force that acts in the plane of the device. This plane force will be perpendicular to the stripe. The magnetic force in the vertical direction pulls the magnetic bead toward the substrate, while the magnetic force acting on a plane traps the cell in the area above the stripe. The force on a whole cell can be found by combining the effects of all magnetic beads on the cell [13]-[14].

A computational simulation using the CFD ACE+ simulator was conducted to observe the distribution of magnetic field intensity inside and outside the microchannel to infer the effect on the capturing of CTCs. The simulation setup to see the magnetic field intensity, T , a function of distance from the vertically-located base permanent magnets, is shown in Fig. 3.

When this happens, the vector component of the drag parallel to the stripe will push the cell along the stripe and will flow at an angle compared to the unlabeled particles to the drift flow force (F_d), as shown as below [13], [14].

$$\vec{F}_m + \cos \theta \vec{F}_d < 0 \quad (3)$$

2. Microfabrication of Microdevice for CTC Separation

The fabrication process was designed to be sufficiently simple and suitable for mass produced protocols [1822]-[2125]. We fabricated the microdevice using inlaid v-shaped ferromagnetic wires with a flat zone, and 6'-wafer level microfabrication processes, including the fluidic control system, using clean room facilities of the MEMS Fab center at ETRI. The microdevices consist of a bottom glass substrate (Boro33 glass wafer) with electroplated Ni-Co (70:30) ferromagnetic wires and a polydimethylsiloxane (PDMS, Sylgard 184, Dow Corning) top substrate with microchannels. To make the ferromagnetic nanowires, a Ti/Cu/Cr (50/200/100 nm) seed layer is deposited, photolithographically patterned, and etched. In addition, a SU-8 photoresist was also spin-coated and patterned photolithographically, exposing only the seed patterns to electroplating. We carried out electroless nickel-cobalt alloy plating, in which nickel and cobalt are deposited onto the conducting surfaces from a hot aqueous solution. After the electroplating, we conducted a chemical-mechanic polishing (CMP) process to achieve a smooth surface with recessed nickel-cobalt stripes, 60- μm thick, with their surfaces planar with the glass surface (Fig. 2b).

To permanently seal the epoxy (SU-8) microfluidic bottom plates and a PDMS chip with microfluidic channels without the use of conventional adhesives, the PDMS surface was amino functionalized after being oxidized through oxygen

plasma treatment to generate silanol (Si-O-H) groups, and then coated with 5% 3-aminopropyltrimethoxysilane (APTMS) in a 95% ethanol (5/95 water/ethanol (v/v)) solution. The PDMS chip, which generated an amino functional group on the surface, was aligned with a bottom plate and then heated at 80–100 °C for 30 min. This method is based on the introduction of amine groups onto the surface of one material, and epoxy groups on other materials, enabling an amine–epoxide polyaddition reaction at their closely contacted solid-to-solid interface to establish covalent and permanent bonding [2226]-[2428]. The microfabricated device (2.5 cm x 7.5 cm x 0.6 cm) with inlaid v-shaped ferromagnetic wires with a flat zone, including a fluidic control system, is shown in Fig. 2.

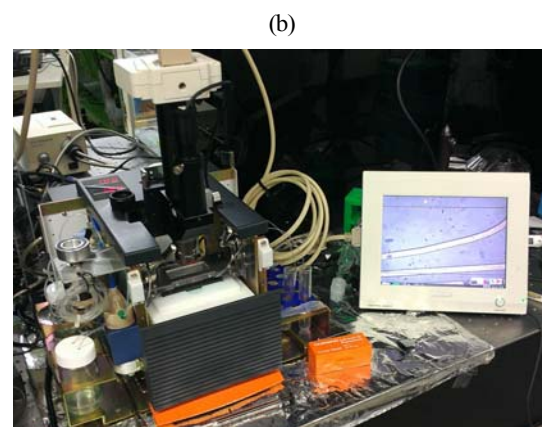
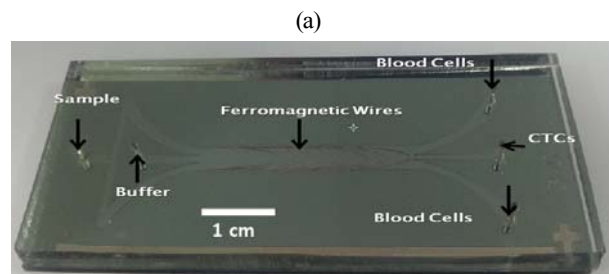
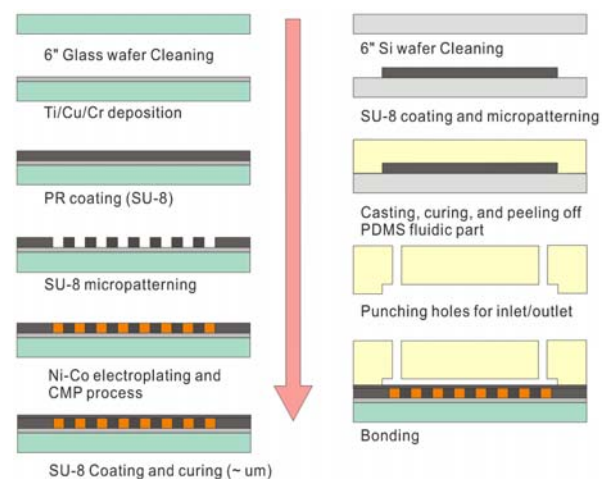


Fig. 2. (a) Microfabrication sequence of the microdevice and (b) photographs of the microdevice ($75\text{ mm} \times 25\text{ mm} \times 6\text{ mm}$) for isolation of CTCs from whole blood. The microchannel has a height of $50\text{ }\mu\text{m}$ and a width of 3 mm at the main flow path, and contains (b) inlaid ferromagnetic wires and (c) a lab-made fluidic control system ($30\text{ cm} \times 20\text{ cm} \times 45\text{ cm}$).

3. Blood Collection, Cell Culture, and Labeling

Healthy human peripheral blood samples were drawn from healthy donors using a protocol approved by the Institutional Review Board (IRB) of Eulji University Hospital, South Korea. Blood samples were collected in Vacutainer™ tubes (BD, Franklin Lakes, NJ) containing EDTA and processed within 3 h.

Cell culture reagents were purchased from GIBCO Invitrogen, Co., unless otherwise specified. MCF-7 was cultured in an RPMI-1640 medium containing 10% fetal bovine serum and a 1% penicillin-streptomycin solution. When the cells reached more than 70-80% confluence, they were collected. For visualization of the cells, they were labeled with Hoechst 33342 (Invitrogen, live cell DNA staining) and calcein-AM (Invitrogen, live cell staining).

4. CTCs Sample Preparation and Separation Process

To determine the separation efficiency of the microdevice, blood samples from healthy donors were spiked with a breast cancer cell line (MCF-7). 5000 or 10000 of MCF-7, which were double labeled with Hoechst 33342 and calcein-AM, were mixed with whole blood at a volume ratio of 1:1. Magnetic-nanobeads coated with an Ep-CAM antibody (Miltenyi biotec, Catalog #: 130-061-101 CD326(EpCAM) MicroBeads, human) were mixed with the prepared blood samples and then incubated for 30 min at room temperature. Even though the size information of nanomagnetic beads is not given in the given data sheet, we have measured the bead size though TEM (is not shown here). The bead sizes is approximately 50 nm (from $25 \sim 75\text{ nm}$). At our experimental setup, when we increased the size of the magnetic beads to $1\text{ }\mu\text{m}$ in diameter, the magnetic beads had a tendency to be easily attached to the magnetic wire patterns, resulting in decreasing the recovery efficiency.

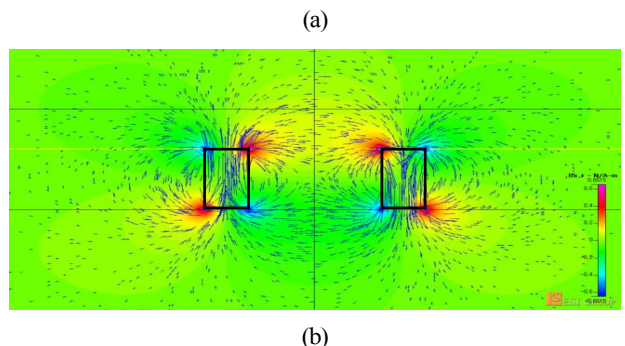
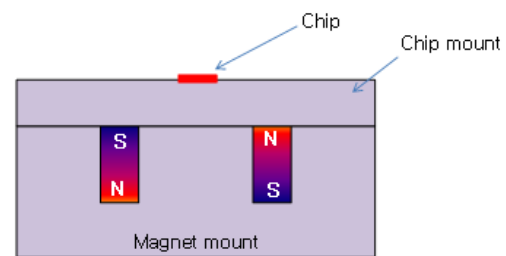
Two syringe pumps were used to inject the blood sample and PBS buffer at 40 and $100\text{ }\mu\text{L}/\text{min}$ flow rates, respectively, into the inlets. The microdevice was placed under a microscope (home-made or Nikon Eclipse LV150) with a fluorescence detector to capture images of cells passing through the microchannel. The separated cells were collected from the center outlet of the microdevice into a 1.5 mL EP tube and

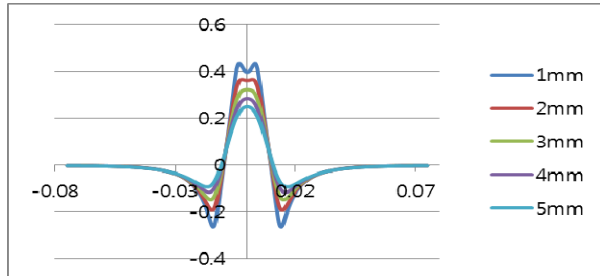
enriched by 500 g of centrifugation for 5 min . The cells were counted using a hemocytometer with a fluorescence microscope.

III. Results and discussion

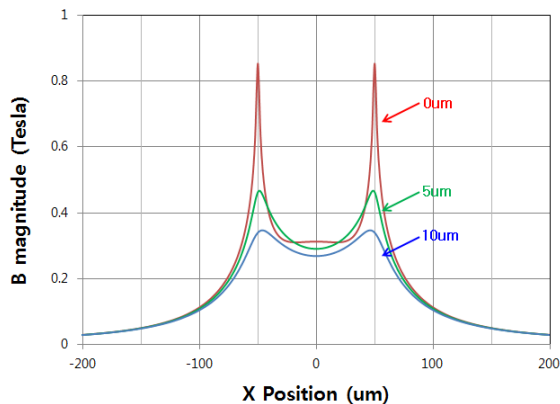
1. Simulation Results

The simulation results from viewing the magnetic field intensity, T , a function of distance ($1, 2, 3, 4$, and 5 mm) from the vertically-located base permanent magnets, are shown in Fig. 3. This result shows that there are areas with an even magnetic intensity between the vertically-located base permanent magnets at various gap conditions. Thus, it provides a tip for where the microchannels are located. In addition, a simulation of the magnetic field intensity as a function of distance ($0, 5$, and $10\text{ }\mu\text{m}$) from the $100\text{ }\mu\text{m}$ -wide ferromagnetic micropattern surface within the microfluidic channel and its results was set up and carried out, as shown in the Supporting Information section Fig. 3. (d). The gradient B distribution of the magnetic field intensity is very intense at the edge of the ferromagnet wires. Based on these results, we can infer that the pattern and its edge design are very important. The separation experiments were carried out using lateral magnetophoresis as a function of distance from the ferromagnetic pattern surface within the microfluidic channel.





(c)



(d)

Fig. 3. (a) Simulation setup for magnetic field intensity (T), which is a function of distance (1~5 mm) from the vertically-located base permanent magnets, and (b) its results ,and (c) distribution of magnetic field intensity (x-axis scale, mm), and (d) distribution of magnetic field intensity (x-axis scale, mm) as a function of distance (0, 5, and 10 μm) from the 100 μm -wide ferromagnetic pattern surface within the microfluidic channel. The blue rectangle is the external magnet bar.

2. Application of Microdevice in CTC Separation

A stack of two neodymium–iron–boron (NeFeB) permanent magnets was placed underneath the CTC microseparator, generating an external magnetic flux of 0.2 T, which was applied in a horizontal direction to the microchannel. CTCs with bound magnetic nanobeads were then drawn laterally along the edge of the wire; meanwhile, normal blood cells flowed into the side outlets, as shown in Fig. 1. The CTCs moving along the wire had no sooner reached the winding point of the wire than they followed the flow direction and flowed into the center outlet for the CTCs. Compared with other lateral magnetophoretic devices with a thin film magnetic wire, it would provide very strong saturated magnetic force to drag and capture the magnetic nanobead-tagged CTCs [13]. In other lateral magnetophoretic devices having magnetic wires in

a shape similar to the teeth of a comb [13], [14], [2529], the CTCs can trap and experience a vortex flow at the microchannel walls, in which the shear stresses are at maximum and there is in no flow slip condition with a buffer solution, i.e., a typical Newtonian flow [2630]-[3228]. Thus, our microdevice with v-shaped magnetic wires guides the CTCs into the center of the flow in the microchannel, and reduces the effects from the wall conditions on the separation of CTCs, thereby reducing the cell loss and enhancing the separation efficiency.

We experimentally observed the isolation of CTCs through path changes of CTC with nano-magnetic beads using a microscope. During the injection of the blood sample, the cells that flowed into the center outlet for the CTCs were recorded through a fluorescence microscope and collected in a 1.5 mL tube, as shown in Fig. 4(b). Real captured photographs showed that the separation of cancer cells (MCF-7) from the whole human blood works well.

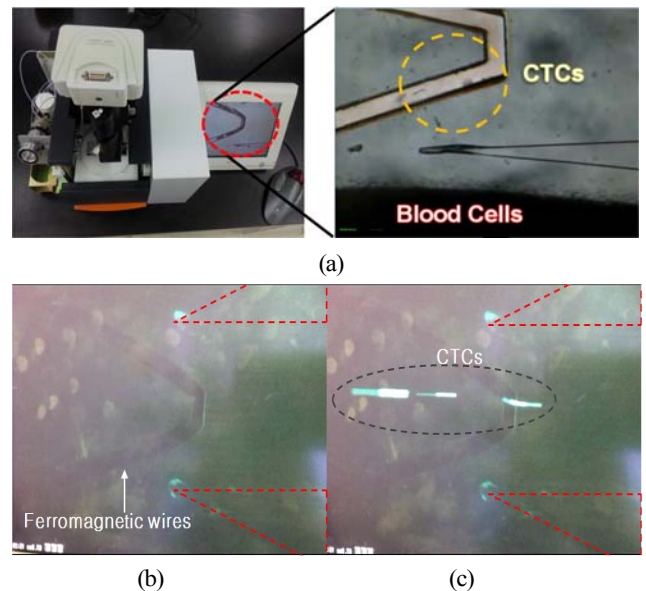


Fig. 4. (a) The proposed device and captured CCD images and (b), (c) fluorescence photographs showing the separation of CTCs using whole human blood with the CTCs flowing into the collection outlet.

Next, the effect of the external static magnetic intensity in the microdevice on the separation rates is shown in Fig. 5. The microdevice shows the maximum separation rate at around an external static magnetic intensity of 180 mT. In addition, we showed that microdevices separated about 93% of the spiked cancer cells (MCF-7) in whole human blood at a flow rate of 40/100 $\mu\text{L}/\text{min}$ with respect to the whole human blood/buffer

solution, as shown in Fig. 6. In addition, the microdevice can purify to over 90%. A peristaltic micropump is utilized to control the flow rate while reducing the flow fluctuation in the fluid. The isolation speed is quite fast, taking 10 min for 400 μL of whole human blood for the overall separation of CTCs, which is suitable for point of care applications. We believe that our microfluidic and microfabricated CTC separation device technology can provide a useful means for prognosis checkups and early screening of breast cancer patients in the form of an in-vitro diagnostics platform in point of care applications.

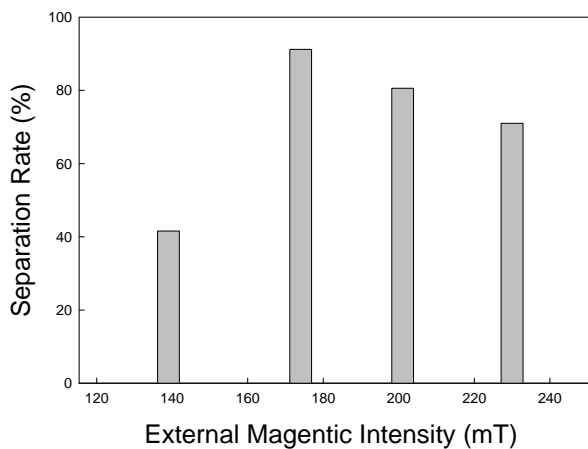


Fig. 5. CTC separation rate of the microdevice as a function of external magnetic intensity.

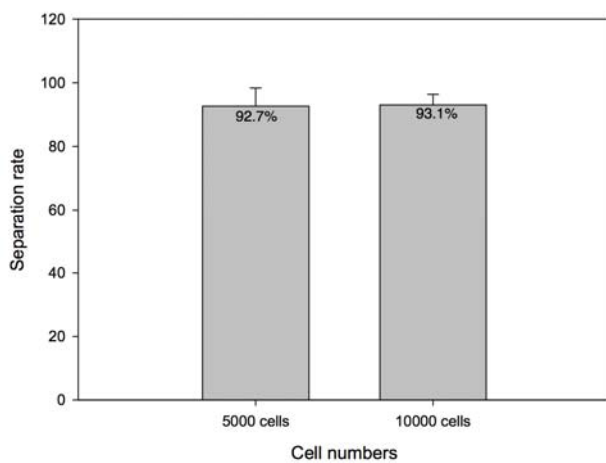


Fig. 6. CTC recovery efficiency of the microdevice using lateral magnetophoresis at an external magnetic field of about 180 mT.

As future work, we are planning to conduct research on applying the device to real cancer patient samples. Furthermore,

the fabricated microstructures may be applicable to a rare cell separation and analysis system or cell-based biosensor systems [2832]-[3135].

IV. Conclusions

We designed and fabricated a microdevice for separation of CTCs from whole human blood based on the principle of lateral magnetophoresis and immunomagnetic nanobeads with EpCAM antibodies that selectively bind to epithelial cancer cells. We designed damascene v-shaped 60 μm -thick Ni-Co ferromagnetic wires with a flat zone and fabricated through micromachining technologies. The isolation condition is stimulated using magnetic field gradient-based isolation technologies. First, we experimentally observed the effect of external static magnetic intensity on the isolation rates. The microdevice with v-shaped embedded magnetic wires guides the CTCs into the center of the flow in the microchannel, reducing the microfluidic CTCs-trapping phenomena at the microchannel walls and enhancing the separation efficiency of the CTCs. Thus, the microdevice was shown to separate about 93% of the spiked CTCs cancer cells (MCF-7) in whole human blood at a flow rate of 40/100 $\mu\text{L}/\text{min}$ with respect to the whole human blood/buffer solution. Microfluidic devices with Ni-Co soft magnetic nanowires combined with a lab-made fluidic control system are very useful for the precise and reliable microfluidic separation of CTCs in an integrated diagnostic instrument. Thus, for the overall isolation, it takes 10 min to process and analyze 400 μL of whole human blood. Since the microfabrication protocols are quite simple and mass-producible, the microdevice can provide a useful and practical means for monitoring the prognosis and early screening of cancer patients in in-vitro diagnostics. Microchips for separating CTCs are applicable to a platform for cancer prognosis, diagnosis of minimal residual diseases, the assessment of tumor sensitivity to anticancer drugs, and personalized anticancer medicines.

References

- [1] S. J. Cohen et al., "Relationship of circulating tumor cells to tumor response, progression-free survival, and overall survival in patients with metastatic colorectal cancer," *Journal of Clinical Oncology*, vol. 26, Jul. 2008, pp. 3213-3221.
- [2] W. He et al., "Quantitation of circulating tumor cells in blood samples from ovarian and prostate cancer patients using tumor-specific fluorescent ligands," *International Journal of Cancer*, vol. 123, Oct. 2008, pp. 1968-1973.
- [3] M. C. Miller, G. V. Doyle and L. W. M. M. Terstappen,

- "Significance of circulating tumor cells detected by the CellSearch system in patients with metastatic breast colorectal and prostate cancer," *Journal of Oncology*, vol. 2010, Jan. 2010, pp.1-8.
- [4] M. Cristofanilli et al., "Circulating tumor cells, disease progression, and survival in metastatic breast cancer," *New England Journal of Medicine*, vol. 351, Aug. 2004, pp.781-791.
- [5] J. S. de Bono et al., "Circulating tumor cells predict survival benefit from treatment in metastatic castration-resistant prostate cancer," *Clinical Cancer Research*, vol. 14, Oct. 2008, pp. 6302-6309.
- [6] C. Alix-Panabieres, S. Riethdorf, and K. Pantel, "Circulating tumor cells and bone marrow micrometastasis," *Clinical Cancer Research*, vol. 14, Aug. 2008, pp. 5013-5021.
- [7] B. Mostert et al., "Circulating tumor cells (CTCs): Detection methods and their clinical relevance in breast cancer," *Cancer Treatment Reviews*, vol. 35, Mar. 2009, pp. 463-474.
- [8] S.K. Arya, B. Lim, and A.R.A. Rahman, "Enrichment, detection and clinical significance of circulating tumor cells," *Lab on a Chip*, vol. 13, Nov. 2013, pp.1995-2027.
- [9] S. Riethdorf et al., "Detection of circulating tumor cells in peripheral blood of patients with metastatic breast cancer : A validation study of the cellsearch system," *Clinical Cancer Research*, vol.13, Feb. 2007, pp. 920-928.
- [10] K.A. Hyun and H.I. Jung, "Advances and critical concerns with the microfluidic enrichments of circulating tumor cells," *Lab on a chip*, vol.14, Jan. 2014, pp.45-56.
- [11] C. Alix-Panabieres and K. Pantel, "Technologies for detection of circulating tumor cells : facts and vision," *Lab on a chip*, vol. 14, Jan. 2014, pp. 57-62.
- [12] S. Nagrath et al., "Isolation of rare circulating tumor cells in cancer patients by microchip technology," *Nature*, vol. 450, Dec. 2007, pp.1235-1239.
- [13] J.D. Adams, U. Kim, and H.T. Soh, "Multitarget magnetic activated cell sorter," *Proceedings of the National Academy of Sciences of the United States of America*, vol. 105, Nov. 2008, pp. 18165-18170.
- [14] S. Kim et al., "Circulating Tumor Cell Microseparator Based on Lateral Magnetophoresis and immuno-magnetic Nanobeads," *Analytic Chemistry*, vol. 85, Feb. 2013, pp. 2779-2786.
- [15] K.A. Hyun et al., "Microfluidic flow fractionation device for label-free isolation of circulating tumor cells (CTCs) from breast cancer patients," *Biosen. Bioelec.*, vol. 40, Feb. 2013, pp.206-212.
- [16] T. Huang et al., "Highly sensitive enumeration of circulating tumor cells in lung cancer patients using a size-based filtration microfluidic chip," *Biosen. Bioelec.*, vol. 51, Jan. 2014, pp.213-218.
- [17] A. Salmanzadeh et al., "Isolation of rare cells through their dielectrophoretic signature," *J. Membra. Sci. Technol.*, vol. 3, Jan. 2013, 1000e112.
- [18] E. Sollier, et al., "Size-selective collection of circulating tumor cells using Vortex technology", *Lab. Chip*, vol. 40, Jan. 2014, pp. 63-77.
- [1519] M. Duch et al., "Development and characterization of Co-Ni Alloys for Microsystems Applications," *Journal of Electrochemical Society*, vol. 149, Feb. 2002, pp. C201-C208.
- [1620] W.P. Taylor et al., "Electroplated soft magnetic materials for microsensors and microactuators," in *Proceedings of the International Conference on Solid-state Sensors and Actuators, Transducer'97*, Chicago, 1997, pp. 1445-1448.
- [1721] B. Lochel and A. Maciossek, "Electrodeposited Magnetic Alloys for Surfac Micromachining," *Journal of Electrochemical Society*, vol. 143, Oct. 1996, pp. 3343-3348.
- [1822] D.-S. Lee et al., "Construction of Membrane Sieves Using Stoichiometric and Stress-Reduced $\text{Si}_3\text{N}_4/\text{SiO}_2/\text{Si}_3\text{N}_4$ Multilayer Films and Their Applications in Blood Plasma Separation," *ETRI Journal*, vol. 34, Apr. 2012, pp. 226-234.
- [1923] S.E. Moon et al., "Semiconductor-Type MEMS Gas Sensor for Real-Time Environmental Monitoring Applications," *ETRI Journal*, vol. 35, Aug. 2013, pp. 617-624.
- [2024] M.S. Kim et al., "SSA-MOA: a novel CTC isolation platform using selective size amplification (SSA) and a multi-obstacle architecture (MOA) filter," *Lab on a Chip*, vo1. 12, May 2012, pp. 2874-2880.
- [2125] D.-S. Lee et al., "Fabrication of Microdevices for Separation of Circulating Tumor Cell Using Lateral Magnetophoresis and Immunomagnetic Nanobeads," *Proceeding of IEEE Sensors Conference*, 2013, pp. 1299-1302.
- [2226] Z. Zhnag, P. Zhao, and G. Xiao, "The fabrication of polymer microfluidic devices using a solid-to-solid interfacial polyaddition," *Polymer*, vol. 50, Sep. 2009, pp. 5358-5361.
- [2327] J.M.K. Ng et al., "Components for integrated poly(dimethylsiloxane) microfluidic systems," *Electrophoresis*, vol. 23, May 2002, pp. 3461-3473.
- [2428] S. Talaei et al., "Hybrid microfluidic cartridge formed by irreversible bonding of SU-8 and PDMS for multi-layer flow applications," *Procedia Chemistry*, vol. 1, Jan. 2009, pp. 381-384.
- [2529] D.W. Inglis et al., "Continuous microfluidic immunomagnetic cell separation," *Applied Physics Letters*, vol. 85, Nov. 22, pp. 5593-5595.
- [2630] S.L. Stott et al., "Isolation of circulating tumor cells using a microvortex-generating herringbone-chip," *Proceedings of the National Academy of Sciences of the United States of America*, vol. 107, Oct. 2010, pp. 18392-18397.
- [2731] A.S.W. Ng et al., "Electrokinetic generation of microvortex patterns in a microchannel liquid flow," *Journal of Micromechanics and Microengineering*, vol. 14, no. 2, pp. 247-253.
- [2832] G.T.A. Kovacs, *Micromachined Transducers Sourcebook*, McGraw-Hill, Chapter 9, 1999, pp.779-883.
- [2933] P. Chen et al., "Multiscale immunomagnetic enrichment of circulating tumor cells:from tubes to microchips," *Lab on a chip*, vol. 14, Feb. 2014, pp. 446-458.
- [3034] B. Hong and Y. Zu, "Detecting Circulating Tumor Cells:

Current Challenges and New Trends," *Theranostics*, vol. 3, no.6, Apr. 2013, pp. 377-394.

[3135] D.R. Parkinson et al., "Considerations in the development of circulating tumor cell technology for clinical use," *Journal of Translational Medicine*, vol. 10, no.138, Oct. 2012, pp. 1-20.